AIP | Applied Physics Letters

Complex quantum transport in a modulation doped strained Ge quantum well heterostructure with a high mobility 2D hole gas

C. Morrison, C. Casteleiro, D. R. Leadley, and M. Myronov

Citation: Applied Physics Letters **109**, 102103 (2016); doi: 10.1063/1.4962432
View online: http://dx.doi.org/10.1063/1.4962432
View Table of Contents: http://scitation.aip.org/content/aip/journal/apl/109/10?ver=pdfcov
Published by the AIP Publishing

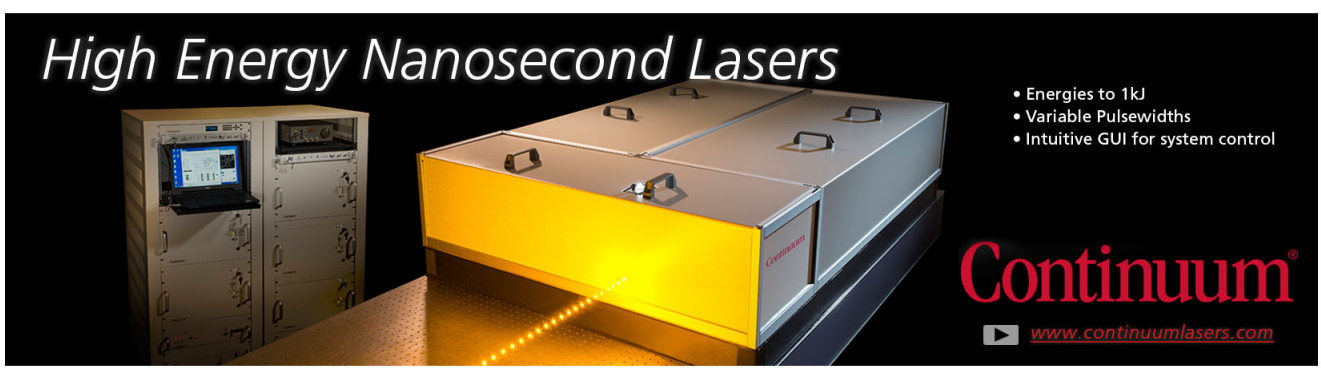

Complex quantum transport in a modulation doped strained Ge quantum well heterostructure with a high mobility 2D hole gas

C. Morrison,[a] C. Casteleiro, D. R. Leadley, and M. Myronov
Department of Physics, University of Warwick, Coventry CV4 7AL, United Kingdom

(Received 27 May 2016; accepted 26 August 2016; published online 7 September 2016)

The complex quantum transport of a strained Ge quantum well (QW) modulation doped heterostructure with two types of mobile carriers has been observed. The two dimensional hole gas (2DHG) in the Ge QW exhibits an exceptionally high mobility of 780 000 cm^2/Vs at temperatures below 10 K. Through analysis of Shubnikov de-Haas oscillations in the magnetoresistance of this 2DHG below 2 K, the hole effective mass is found to be 0.065 m_0. Anomalous conductance peaks are observed at higher fields which deviate from standard Shubnikov de-Haas and quantum Hall effect behaviour due to conduction via multiple carrier types. Despite this complex behaviour, analysis using a transport model with two conductive channels explains this behaviour and allows key physical parameters such as the carrier effective mass, transport, and quantum lifetimes and conductivity of the electrically active layers to be extracted. This finding is important for electronic device applications, since inclusion of highly doped interlayers which are electrically active, for enhancement of, for example, room temperature carrier mobility, does not prevent analysis of quantum transport in a QW. *Published by AIP Publishing.* [http://dx.doi.org/10.1063/1.4962432]

Epitaxially grown Ge is of great interest for device applications, primarily due to its high hole mobility[1,2] and compatibility with epitaxial Si technology. Recently, epitaxially grown layers of Ge grown on SiGe on a standard Si(001) substrate have been shown to have extremely high room temperature hole mobility of up to 4500 cm^2/Vs due to formation of a two dimensional hole gas (2DHG).[2,3] Compressive strain of the Ge epilayer induced by epitaxial growth results in 2DHG formation and the holes have enhanced mobility due to their lower effective mass and reduced scattering factors. Low temperature 2DHG mobility in excess of 1.3×10^6 cm^2/Vs has been achieved.[1,4–6] The study of quantum transport behaviour in these 2DHGs at low temperatures, in particular, the Shubnikov de-Haas (SdH) oscillations that arise from Landau levels created under an applied magnetic field, allows us to determine the key parameters such as effective mass, as well as the carrier densities and diffusive and quantum transport scattering parameters.

Previously, low temperature magnetotransport has been studied for Ge quantum wells (QWs) but primarily on structures with comparatively low 2DHG mobility and much higher carrier densities.[7–10] For example, Miura *et al.* studied quantum transport in a compressively strained Ge QW with a 2DHG mobility of 23 800 cm^2/Vs and a carrier density of 2.4×10^{12} cm^{-2}.[11] Prior to the recent report of hole mobility in excess of 1×10^6 cm^2/Vs at a carrier density of 2.9×10^{11} cm^{-2} in a Ge QW,[1] the record value of mobility was 120 000 cm^2/Vs with a carrier density of 8.5×10^{11} cm^{-2}.[12] The study of quantum transport in high mobility Ge 2DHGs since this discovery has primarily focussed on the spin-orbit interaction in heterostructures of this type[13–15] and on the composite fermions and the fractional quantum Hall effect in high magnetic fields.[4–6] Here, we study low temperature quantum transport in a Ge QW heterostructure, modulation doped with 2×10^{18} cm^{-3} of boron (B) and a delta layer of B. This doped heterostructure has a low temperature hole mobility of 780 000 cm^2/Vs, approaching the record value.

The heterostructure studied here was grown by reduced pressure chemical vapor deposition onto a 100 mm n-type Si (001) substrate. The structure is shown schematically in Figure 1, and the corresponding band structure simulated using a Poisson-Schrödinger method may be found in the study by Foronda *et al.*, Figure 3.[14] A reverse linearly graded (RLG) buffer layer was first grown onto the substrate, followed by the active region. A doping concentration of 2×10^{18} cm^{-3} B was created in the supply layer and a delta layer of B directly below this layer. The delta layer was inserted to maximise the room temperature 2DHG mobility to 4500 cm^2 V^{-1} s^{-1} in this Ge QW.[2] However, because the

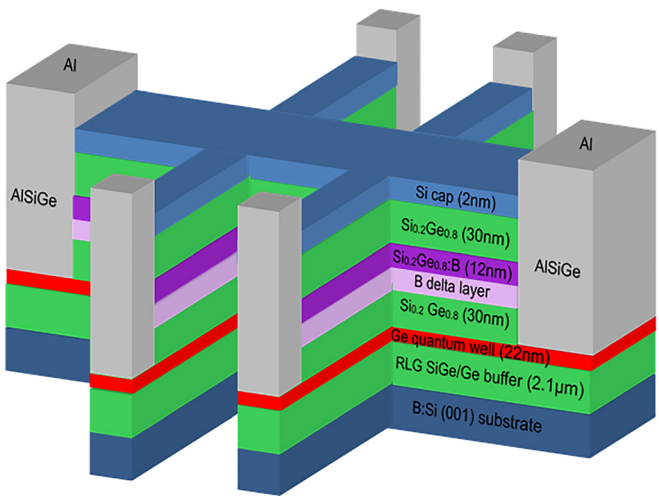

FIG. 1. (a) Schematic of the Ge quantum well heterostructure studied here, showing the Hall bar geometry used for the magnetotransport measurements. The primary active transport layer (location of the 2DHG) is indicated in red.

[a]Author to whom correspondence should be addressed. Electronic mail: c.morrison.2@warwick.ac.uk

boron doping level in the delta layer is above the metal-insulator transition it will be conductive even at very low temperatures and cause deviations from the norm in quantum phenomena like Shubnikov de-Haas oscillations in the magnetoresistance and the quantum Hall resistance plateaus at low temperatures. The density of Boron in the delta doped region was determined to be $5 \times 10^{18}\,\mathrm{cm}^{-3}$ using Secondary Ion Mass Spectrometry (SIMS). The thicknesses of the layers were confirmed by cross-sectional transmission electron microscopy. A detailed study of the material properties of this heterostructure has been published elsewhere.[3]

Magnetotransport, Hall effect, and resistivity measurements were performed using a Hall bar geometry produced using photo-lithography. Thermally evaporated Al was used as a contact material, post-annealed to form a contact with the QW. The Ge QW mesa was defined by reactive ion etching in an SF_6:O_2 mixture down to the Si substrate. All contacts were found to exhibit Ohmic behaviour at 20 K and below, with typical contact resistances between 400 Ω and 1000 Ω at 20 K. All magnetotransport measurements were performed using an ac current excitation of 100 nA at a frequency of 19.77 Hz. The magnetic field was applied perpendicular to the plane of the device. Sheet resistance and Hall coefficient were measured from room temperature down to 0.3 K, from which the sheet carrier density and Hall mobility were calculated. Carrier freeze-out does not occur at low temperatures, and the Ge QW demonstrates good, metallic transport behaviour indicative of the presence of 2D confinement. Mobility at the lowest temperatures is very high ($780\,000\,\mathrm{cm}^2/\mathrm{Vs}$), approaching the record value in this class of heterostructures.[1] The carrier density is $2 \times 10^{11}\,\mathrm{cm}^{-2}$ at 0.3 K, indicating a relatively high transferal of carriers from the doping layer into the QW region.

Magnetotransport and Hall effect measurements were made under an applied magnetic field B of up to 12 T perpendicular to the Hall bar, for temperatures T from 300 mK up to 10 K. The results at 338 mK are shown in Figure 2; the data shown in the figure represent the average of the magnetoresistance and Hall resistance magnitudes across both magnetic field polarities. Clear SdH oscillations are observed; however, the oscillatory behavior is unusually complex due to the presence of two parallel conducting layers: at the lowest temperatures, there are SdH minima corresponding to the even integer filling factor at low B; above 0.3 T, odd integer SdH minima also appear due to Zeeman splitting; however, above about 0.6 T, sharp peaks at all integer filling factors start to dominate the resistivity. As the temperature is increased, the transition from minima to maxima at the integer filling factor moves to higher B and the amplitude of the peaks decreases. These peaks cannot be explained by conventional Shubnikov de-Haas theory of a single carrier type. The Hall resistance is also complex, with no observable quantum Hall plateaus and instead sharp minima occurring in the Hall resistance at the integer filling factor, with temperature dependent amplitude. By plotting the magnetoconductance of the structure instead it is possible to isolate the conductance due to parallel conduction in the heterostructure. This quantity is plotted in Figure 3 for the lowest temperature studied (338 mK), again averaged across both polarities of magnetic field. The dashed orange line indicates

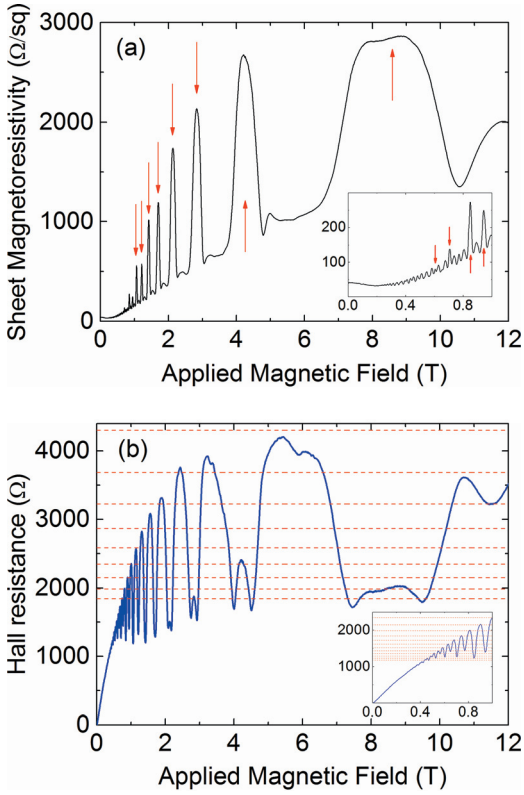

FIG. 2. (a) Magnetoresistance and (b) Hall effect measurement at 338 mK for the B modulation doped 2DHG for an applied magnetic field up to 12 T, showing the magnitude of the magnetoresistance and Hall resistance averaged across both magnetic field polarities. Insets: resistance data at low fields. Red arrows indicate the position of anomalous resistance peaks. Red dashed lines indicate the expected position of integer quantum Hall plateaus.

the base conductance (30 μS) of the layers conducting in parallel to the 2DHG, which may be compared to the much larger conductance of 24 900 μS in the QW. This corresponds to only 0.1% electrical conductance via the B delta layer. Most of the layers in the heterostructure are intentionally undoped and therefore are unlikely to form a parallel conduction channel at low temperatures due to carrier freeze-out. We therefore suggest that the main source of conduction parallel to the 2DHG is in the B modulation doping

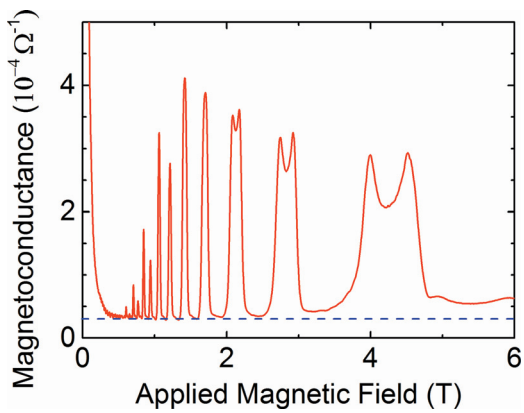

FIG. 3. Magnetoconductance at 338 mK, averaged across both magnetic field polarities. The dashed blue line shows background conductance as a result of parallel conduction in the region of the doping layer. The conductance of the parallel conduction layer is 30 μS and therefore the conductance in the 2DHG only may be calculated as 24 900 μS. The parallel conductance is only 0.1% of the total conductance of the heterostructure.

delta layer. Due to the high carrier occupation remaining in this region, we may conclude that we have achieved the limit of 2DHG carrier density in the QW achievable by modulation doping for a given amount of biaxial compressive strain and consequently the valence band offset of the Ge QW. Increasing the strain present in the QW region by, for example, reducing the percentage of Ge in the buffer layer is expected to increase the carrier density limit in the 2DHG. This has the additional advantage of increasing the energy gap between the heavy and light hole bands and consequently reducing interband scattering, which would result in a further increase of hole mobility in the 2DHG.

By plotting the inverse field position of the minima/maxima in the magnetoresistance as a function of quantum Hall filling factor, it is possible to extract the sheet carrier density of the 2DHG producing the oscillations. This plot is shown in Figure 4 for the lowest temperature (338 mK). The gradient of this curve is equal to $\frac{hp}{e}$, where p is the sheet hole density of the 2DHG. Performing a linear fit to the data in Figure 4 gives a sheet hole density of $2.0 \times 10^{11}\,\mathrm{cm}^{-2}$. This value agrees with the sheet carrier density calculated using the low field Hall resistance as previously shown. This analysis shows that, despite the apparently complex oscillatory behaviour observed, all the oscillations arise due to the existence of Landau levels created from a single, fundamental energy level in the QW.

The peaks in magnetoresistance as a function of magnetic field in the low field regime may be used to calculate the effective mass of carriers in the conduction region(s) by an iterative process. The analytical equation that describes Shubnikov-de Haas oscillations is as follows:[16,17]

$$\frac{\Delta\rho_{xx}(B)}{\rho_{xx}(0)} = 4\cos\left(\frac{2\pi E_F m^*}{\hbar eB}\right)\exp\left(-\frac{\pi m^*\alpha}{eB\tau_t}\right)\frac{\psi}{\sinh(\psi)}, \quad (1)$$

where E_F is the Fermi energy, α is the Dingle ratio ($\frac{\tau_t}{\tau_q}$, where τ_t is the transport scattering time and τ_q is the quantum scattering time), and $\psi = \frac{2\pi^2 k_B T m^*}{\hbar eB}$.

Plots of two simultaneous equations derived from this equation that may be used to iteratively solve for the effective mass and Dingle ratio are shown in Figure 5.[18] These plots represent the final iteration of the solution using an iterative step of 0.005 m_0. Two clear strata of points are observed, corresponding to carriers with differing quantum lifetimes. We find that a solution is obtained, for both strata analysed individually, for an effective mass $m^* = 0.065\ m_0$. However, the Dingle ratio varies considerably. For the main stratum, illustrated by a black dashed line, the Dingle ratio is found to be 18, increasing to 33 for the second stratum (red dashed line).

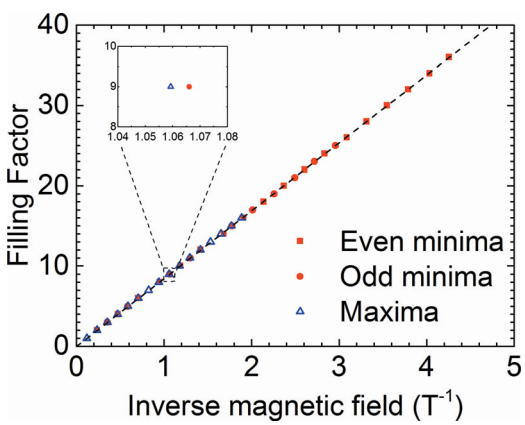

FIG. 4. Plot of inverse field positions of minima/maxima in the magnetoresistance against filling factor, at a temperature of 338 mK. The carrier density extracted from a linear fit to the data is $2.0 \times 10^{11}\,\mathrm{cm}^{-2}$. The inset resolves the separation of maxima and minima in inverse magnetic field space.

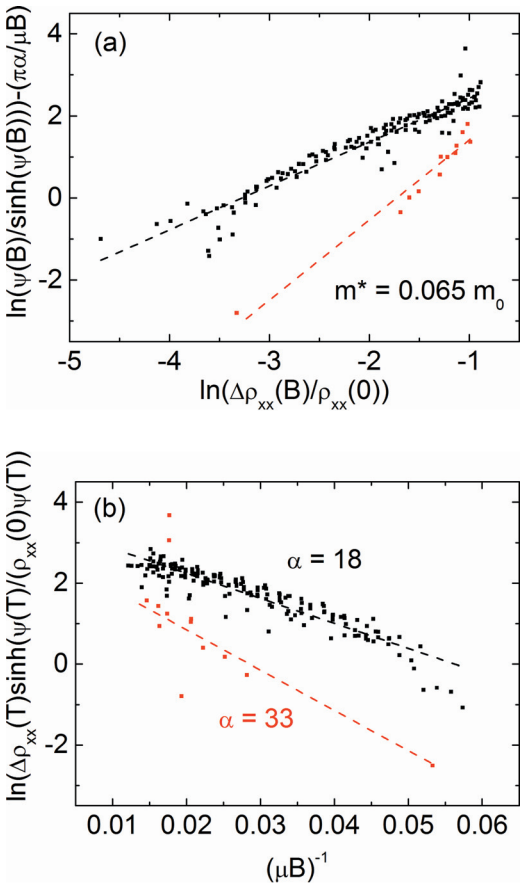

FIG. 5. (a) and (b) Plots of transformed data using Equation (1) for effective mass analysis. Two clear strata are observed on the curve, corresponding to two different Dingle ratios and consequently two different quantum lifetimes; however, both strata correspond to the same effective mass (0.065 m_0).

The transport scattering time for holes in the 2DHG may be calculated using the expression $\tau_t = \frac{m^*\mu_H}{e}$, where μ_H is the Hall mobility. Inserting the Hall mobility at 338 mK ($780\,000\,\mathrm{cm}^2/\mathrm{Vs}$) and the effective mass yields a value of $\tau_t = 29$ ps, corresponding to a transport scattering length of 5.7 μm. Using this value for τ_t and the calculated Dingle ratios gives quantum scattering times $\tau_q = 1.6$ ps, and 0.87 ps for the two carrier lifetimes revealed through the effective mass analysis.

The carrier density of the occupied energy levels in the QW may be calculated from the Shubnikov-de Haas oscillations, by a fast Fourier transform method. First, the oscillatory magnetoresistance behaviour is isolated by subtraction of a quadratic resistance background due to ordinary (geometric) magnetoresistance. These data are then plotted as a function of inverse magnetic field and a fast Fourier transform is performed. The resulting spectrum exhibits peaks at given frequencies (units of T) which correspond to carrier densities in the QW via the relation $p = \frac{fe}{\pi\hbar}$, where f is the frequency of

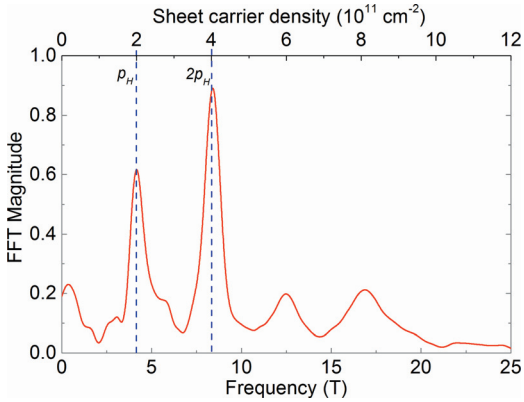

FIG. 6. Fast Fourier transform of the low field (<0.8 T) magnetoresistance at 338 mK as a function of inverse field. The upper x-axis shows the frequency of oscillation transformed into sheet carrier density.

oscillation. The spectrum resulting from transformation of the 338 mK magnetoresistance data, below the first anomalous conductance peak, is shown in Figure 6. Clear peaks are observed at the Hall carrier density (2×10^{11} cm^{-2}) and at twice the Hall carrier density (4×10^{11} cm^{-2}). The second peak may either be a harmonic or be indicative of quantum transport in another layer, for example, the highly B doped SiGe region. However, as shown in Figure 4, all Shubnikov de-Haas maxima/minima can be attributed to Landau levels generated from the Fermi energy for carriers at the Hall carrier density (2×10^{11} cm^{-2}). We can therefore attribute the second peak to harmonic generation due to the onset of Zeeman split peaks. The two additional, lower amplitude peaks at higher carrier densities are further harmonics corresponding to three and four times the first sub-band density, respectively.

Assuming a carrier density of 1×10^{12} cm^{-2} for the delta doped B layer, based on the SIMS-determined dopant density and a typical activation approximately 50%, the background conductivity extracted from Figure 3 gives an approximate value for the mobility of 200 cm^2/Vs at 338 mK. The mobility in this region is primarily limited by the high degree of ionised impurity scattering from acceptor ions, and this value agrees well with the expected value for mobility for Ge at this doping level. For most applications, one does not wish to have a parallel layer as this will complicate device designs and hinder performance. For applications, it is desirable to instead achieve higher carrier density (and mobility) through the use of an electrostatic gate, avoiding the use of dopant layers altogether. In such a structure, a doping layer would in fact hinder gate performance due to screening of the gate potential and is so further undesirable. The findings in this study help in the design of device parameters without requiring a complex gate optimisation process.

In summary, a high mobility (780 000 cm^2/Vs) 2DHG has been created in a strained Ge QW structure, through B modulation doping. The mobility and carrier density were measured through Hall effect measurements at temperatures between 0.3 K and 300 K, revealing a low temperature carrier density of 2×10^{11} cm^{-2}. Low temperature magnetoresistance measurements show a complex Shubnikov de-Haas oscillatory behavior. Analysis of the oscillation amplitudes yields an effective mass $m^* = 0.065\ m_0$. Fast Fourier transform analysis shows peaks at two frequencies, corresponding to carriers at carrier densities of 2×10^{11} cm^{-2} and 4×10^{11} cm^{-2}, respectively. The first peak agrees with the carrier density extracted via Hall effect analysis, and the second peak is a harmonic of the fundamental peak due to Zeeman splitting. The lack of quantum transport in the parallel conduction layer is consistent with the B doping region being too narrow for 2D confinement to occur. A two channel model allows us to extract key electrical parameters including the conductivity of the channels and their respective mobilities. The Hall mobility of the heterostructure corresponds closely to that of the QW alone, due to the large difference in mobilities and conduction being primarily through the QW region. The parallel, low mobility transport channel is consistent with electronic transport by carriers in the highly B doped region of the heterostructure.

This work was supported by the EPSRC funded "Spintronic device physics in Si/Ge Heterostructures" EP/J003263/1 and "Platform Grant" No. EP/J001074/1 Projects.

[1]A. Dobbie, M. Myronov, R. J. H. Morris, A. H. A. Hassan, M. J. Prest, V. A. Shah, E. H. C. Parker, T. E. Whall, and D. R. Leadley, Appl. Phys. Lett. **101**, 172108 (2012).
[2]M. Myronov, C. Morrison, J. Halpin, S. Rhead, J. Foronda, and D. Leadley, Solid-State Electron. **110**, 35 (2015).
[3]M. Myronov, C. Morrison, J. Halpin, S. Rhead, C. Casteleiro, J. Foronda, V. A. Shah, and D. Leadley, Jpn. J. Appl. Phys. **53**, 04EH02 (2014).
[4]Q. Shi, M. A. Zudov, C. Morrison, and M. Myronov, Phys. Rev. B **91**, 201301 (2015).
[5]Q. Shi, M. A. Zudov, C. Morrison, and M. Myronov, Phys. Rev. B **91**, 241303 (2015).
[6]Q. Shi, M. A. Zudov, C. Morrison, and M. Myronov, Phys. Rev. B **92**, 161405 (2015).
[7]T. Irisawa, M. Myronov, O. A. Mironov, E. H. C. Parker, K. Nakagawa, M. Murata, S. Koh, and Y. Shiraki, Appl. Phys. Lett. **82**, 1425 (2003).
[8]B. Rößner, G. Isella, and H. V. Känel, Appl. Phys. Lett. **82**, 754 (2003).
[9]K. Sawano, Y. Kunishi, Y. Shiraki, K. Toyama, T. Okamoto, N. Usami, and K. Nakagawa, Appl. Phys. Lett. **89**, 162103 (2006).
[10]Y. F. Komnik, Low Temp. Phys. **32**, 82 (2006).
[11]N. Miura, N. V. Kozlova, K. Dörr, J. Freudenberger, L. Schultz, O. Drachenko, K. Sawano, and Y. Shiraki, J. Low Temp. Phys. **159**, 222 (2010).
[12]B. Rössner, D. Chrastina, G. Isella, and H. von Känel, Appl. Phys. Lett. **84**, 3058 (2004).
[13]C. Morrison, P. Wiśniewski, S. D. Rhead, J. Foronda, D. R. Leadley, and M. Myronov, Appl. Phys. Lett. **105**, 182401 (2014).
[14]J. Foronda, C. Morrison, J. E. Halpin, S. D. Rhead, and M. Myronov, J. Phys.: Condens. Matter **27**, 022201 (2014).
[15]C. Morrison, J. Foronda, P. Wiśniewski, S. D. Rhead, D. R. Leadley, and M. Myronov, Thin Solid Films **602**, 84 (2016).
[16]A. Isihara and L. Smrcka, J. Phys. C: Solid State Phys. **19**, 6777 (1986).
[17]P. Coleridge, R. Stoner, and R. Fletcher, Phys. Rev. B **39**, 1120 (1989).
[18]Y. F. Komnik, V. V. Andrievskii, I. B. Berkutov, S. S. Kryachko, M. Myronov, and T. E. Whall, Low Temp. Phys. **26**, 609 (2000).